Open Archive Toulouse Archive Ouverte (OATAO)

To link to this article:

URL : **http://dx.doi.org/10.1016/j.surfcoat.2009.04.020**

Multilayer chromium based coatings grown by atmospheric pressure direct liquid injection CVD

F. Maury, A. Douard, S. Delclos, D. Samelor, C. Tendero *

CIRIMAT, CNRS/INPT/UPS, ENSIACET, 118 Route de Narbonne, 31077 Toulouse cedex 4, France

A B S T R A C T

There is a great interest for multilayer hard coatings because they exhibit enhanced properties resulting from their nanostructuration. Such coatings are frequently constituted of carbide and nitride and are generally deposited under very low pressure by plasma and PVD processes. These vacuum techniques enable the growth of heterostructures with nanometric thick individual layers and sharp interfaces, which are two requirements for advanced performances. However, both to develop more economical processes and with the goal of continuous deposition applications, the CVD processes operating under atmospheric pressure are particularly attractive. In this paper we show that the combination of pulsed direct liquid injection and the use of metalorganic precursor (DLI-MOCVD) is a promising route for the growth of nanostructured multilayer coatings under atmospheric pressure. Chromium metal as well as chromium carbide and nitrides monolithic coatings have been deposited at 773 K by this process using liquid solution of bis(benzene) chromium as Cr molecular precursor. Then, CrC_x/CrN nanostructured multilayer coatings with a bilayer period as low as 50 nm have been grown. Structural characterizations and preliminary mechanical properties of these metallurgical coatings are discussed.

Keywords:
DLI-CVD
Nanostructured multilayers coatings
CrC/CrN
Atmospheric pressure process

1. Introduction

The need for advanced tribological coatings has pushed the research both on the design of new coatings and on the development of deposition processes. Many commercial coatings are made up of a monolithic layer containing a single phase which is frequently Ti-based or Cr-based materials. The last ones have considerable interest because of their good resistance to wear, corrosion and oxidation. More performing systems consist either of duplex structures combining individual properties of different constituents [1] or of composition gradient layers. The best advances are due to new designs which use the nanostructuration to enhance the properties. There are two major approaches: (i) the nanocomposites coatings where nanocrystallites are embedded in an amorphous matrix [2] and (ii) multilayer coatings where two thin layers of different materials are repeated periodically with a bilayer period as low as few nanometers. The biperiod and the number of interfaces are the most important parameters that influence functional properties of multilayer coatings [3–5].

Multilayers can be divided as isostructural and non-isostructural depending on whether the constituent materials have the same structure or not [6]. Non-isostructural multilayer coatings combine materials which form thermodynamically stable interfaces, e.g. metal/ ceramics [7] and nitride/nitride multilayers [8]. When combining materials with different structures, a layer can crystallize in a metastable

structure in order to form a coherent interface with the other. The stabilization of metastable phases can be observed for nanometric biperiod and was found to enhance hardness and corrosion resistance at high temperature [8]. For isostructural multilayer coatings, epitaxial accommodation at the interfaces leads to the growth of superlattice when the individual layer thickness is in the size of lattice dimension. Then the coating is considered as a new material as demonstrated for TiN/VN [9].

Chromium-based hard coatings are particularly attractive for applications under hostile environment. For instance chromium nitride combined with other transition metal nitrides exhibit superior mechanical and tribological properties as well as higher thermal stability compared to the basic constituents, as shown for CrN/TiN [10], CrN/WN [11], CrN/AlN [8] or CrN/NbN [12,13]. Entirely Cr-based multilayer coatings are of interest because it can simplify the growth process due to the use of a single metal source. They have been deposited by a variety of physical vapor processes (PVD, PLD), i.e. by high vacuum techniques (Table 1). Different phases have been combined as Cr/CrN [4,5,14–18], Cr/CrC_x [19,20], CrN/CrC_x [21], CrN/ Cr_2N [16,22]. For instance, compared to the monolithic layers, Cr/CrC_x multilayer coatings exhibit a lower wear rate [20] and CrN/CrC_x a lower friction coefficient [21]. Superlattice growth was observed only for CrN/CrC_x [21] and Cr/CrC_x [19]. The number of individual layers is typically between 10 and 100 and the biperiod is as low as a few tens of nanometers.

We have previously reported that bis(benzene)chromium (BBC: $Cr(C_6H_6)_2$) was a suitable molecular precursor for the growth at low

* Corresponding author. Tel.: +33 562885678; fax: +33 562885600.
  E-mail address: claire.tendero@ensiacet.fr (C. Tendero).

Table 1
Principal works on Cr-based multilayer coatings showing that the unique process operating at or near atmospheric pressure is DLI-MOCVD.

Multilayer coatings	Deposition process	Bi-period λ (nm)	Number of layers	Reference
Cr/CrN	PVD	11–120	20–160	[4,5]
	PVD	20–100	12–60	[14]
	PVD	40–2300	–	[15]
	PVD	–	2–8	[16]
	PLD	60–1000	2–32	[17]
	PLD	–	4–32	[18]
	DLI-MOCVD	130–271	16–20	[27]
Cr/CrC$_x$	PVD	20–300	10–150	[19]
	PVD	22–150	20–150	[20]
CrN/CrC$_x$	PVD	5–90	20–260	[21]
	DLI-MOCVD	25–204	10–110	This work
CrN/Cr$_2$N	PVD	30–150	10–40	[22]
	PVD	–	2–8	[16]

Multilayer coatings containing alternatively chromium and another transition metal compound are not reported.
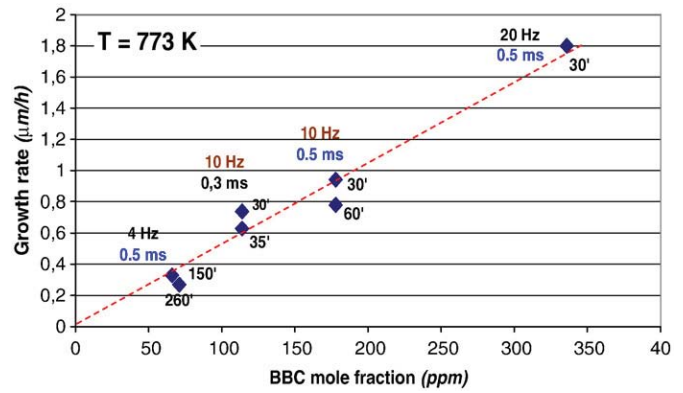

Fig. 1. Influence of the BBC mole fraction on the growth rate of CrC$_x$ coatings. The BBC mole fraction was controlled by the injection parameters (frequency, opening time and deposition time).

temperature of chromium carbide by low pressure MOCVD [23]. Deposition of CrN and Cr metal was also possible using NH$_3$ and C$_6$Cl$_6$ as co-reactant, respectively, still under low pressure [24]. Furthermore, we recently showed using another organochromium compound that pulsed direct liquid injection (DLI) was a convenient technique to feed CVD reactors operating under atmospheric pressure [25]. The motivation of this work is to develop original atmospheric pressure DLI-CVD processes for the growth of Cr-based multilayer hard coatings. Processes operating under atmospheric pressure are particularly attractive for economical reasons and for continuous deposition as on line strip coating. The chemistry of these processes and trends for the growth conditions were determined by thermodynamic calculations using BBC as Cr source and the above mentioned co-reactants in presence of a solvent [26]. The influence of a slight decrease of the total pressure is described in a companion paper [27] and we focus here on results obtained under atmospheric pressure.

2. Experimental

Chromium carbide and nitride as well as metallic chromium are deposited both on silicon and stainless steel by DLI-MOCVD, using BBC as Cr source in reacting mixtures which composition depends on the nature of the targeted coating, as shown in Table 2. Chromium carbide is deposited with toluene/BBC/N$_2$ gas mixture: carbon incorporation results essentially from the decomposition of BBC. When NH$_3$ is added to this mixture, CrN is formed. The addition of C$_6$Cl$_6$ leads to metal chromium deposition: C$_6$Cl$_6$ prevents the carbon incorporation as discussed elsewhere [24].

It is important to note that BBC is a solid Cr(0) molecular compound, free from hexavalent chromium derivative. Toluene was selected as

solvent because it meets the requirements for the DLI-MOCVD process: no interaction with the precursor, high vapour pressure, good thermal stability, low viscosity and surface tension [25]. Moreover toluene belongs to the aromatic family as the benzene ligands of BBC and thereby it should not change drastically the chemistry of the process. Its lower toxicity than benzene is an advantage although new solvents have to be tested for a more environmental friendly process.

The DLI-MOCVD principle is based on the pulse liquid injection of the reacting mixture in a flash vaporization chamber maintained at 473 K to generate the reactive vapour which is carried by a nitrogen stream to the heated substrate where the deposition reaction occurs. Whatever the kind of coating, the deposition was performed at 773 K under atmospheric pressure. The experimental set up is described in details in [25].

The coatings (both monolithic and multilayered) were characterised by FEG-SEM for the morphology, EPMA for the composition, XRD for the crystalline structure and SIMS for the composition depth profile. Preliminary functional properties for further mechanical applications were investigated in terms of thermal stability, nano-hardness and wear resistance.

3. Results and discussion

3.1. Growth of monolithic coatings

CrC$_x$, Cr and CrN monolithic coatings are grown by tuning the reacting mixture, with a deposition rate around a few nanometers per minute. An example of the influence of the injection parameters and the BBC mole fraction on the growth rate is given for CrC$_x$ deposition in Fig. 1. BBC mole fraction increases with the injection parameters (opening time and frequency). This BBC enrichment of the reacting
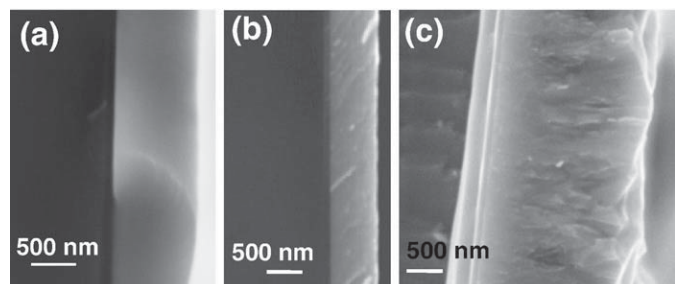
Table 2
Deposition conditions and main features of monolithic Cr-based coatings grown by atmospheric pressure DLI-MOCVD using a BBC solution in toluene (0.03 mol l^{-1}).

Coating	Co-reactant	T (K)	XRD structure	Mean crystallite size[c] (nm)	Composition	Growth rate (nm min^{-1})
CrC$_x$	–	773	Amorphous	–	Cr$_{0.69}$C$_{0.28}$O$_{0.03}$	5.5
Cr	C$_6$Cl$_6$[a]	773	bcc-Cr	8	Cr$_{0.87}$C$_{0.13}$	6.0
CrN	NH$_3$[b]	773	fcc-CrN	12	Cr$_{0.40}$N$_{0.27}$O$_{0.31}$C$_{0.02}$	4.2

Injection conditions range of BBC solution: frequency 4–10 Hz; opening time 0.3–0.5 ms; BBC mole fraction 66–200 ppm.

[a] C$_6$Cl$_6$/BBC = 10%.
[b] NH$_3$/BBC = 280.
[c] Determined using the Scherrer formula from the (200)CrN and (110)Cr XRD peaks.

Fig. 2. SEM micrographs of cross sections of fractured samples grown at 773 K on Si substrates: (a) amorphous CrC$_x$; (b) nanocrystalline Cr; (c) (200) textured CrN.
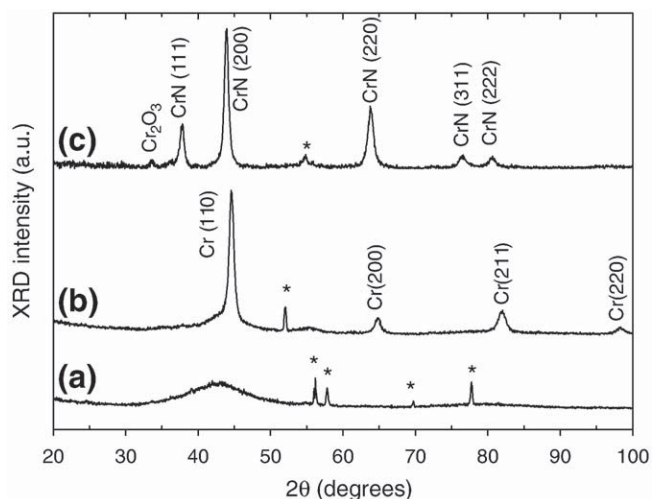
Fig. 3. Grazing angle (2°) XRD patterns of monolithic coatings grown at 773 K on Si substrates: (a) Cr; (b) CrC$_x$; (c) CrN (peaks originating from the substrate are noted with an asterisk).

Fig. 5. SIMS depth composition profile of a CrC$_x$/CrN-10 coating showing the 10 layers grown on Si substrate protected with a Si$_3$N$_4$ thin layer (bi-period 204 nm).

gas phase results in a linear increase of the deposition rate, which indicates that the growth kinetic is controlled by mass transport.

The nature of the coating strongly influences its morphology and crystalline structure, as shown by the SEM and XRD analysis. Figs. 2 and 3 sum up the characteristics of the monolithic coatings.

Chromium carbide film is compact and amorphous: the XRD pattern exhibits a broad peak centered at 42°.

Concerning the chromium coating, which is obtained by adding C$_6$Cl$_6$ to the reacting mixture, the crystalline structure remains bcc (with a size of 8–10 nm for the nanocrystals) in spite of the incorporation of 13 at.% of carbon. Theoretically, only 0.4 at.% of carbon is likely to be solved in the metal structure. As a result it can be considered as a metastable phase. Similar metal coatings with carbon content in the range 8–11 at.% were previously grown by MOCVD [24], i.e. the presence of solvent vapor as in DLI-MOCVD does not influence significantly the carbon content. This carbon excess is both in the form of amorphous free carbon (no evidence of graphite by XRD) and carbide as found by XPS analyses (not shown here). The coating is dense and exhibits a metallic aspect. Its roughness Ra is around 30 nm whereas chromium carbide exhibits a Ra in the range of 50–150 nm.

In NH$_3$ atmosphere, the cubic phase fcc of CrN is deposited. The growth is columnar: this columnar morphology can be clearly observed with SEM when the thickness is higher than approximately 500 nm (Fig. 2c). It is noteworthy that, in this range of thickness (e.g.
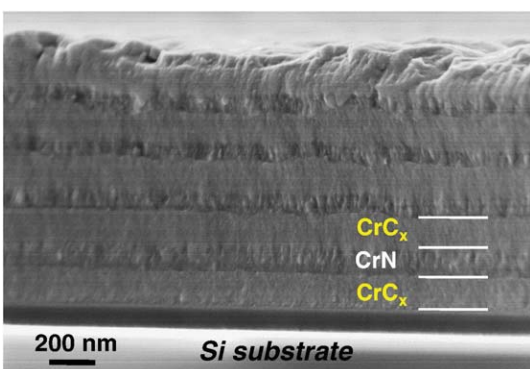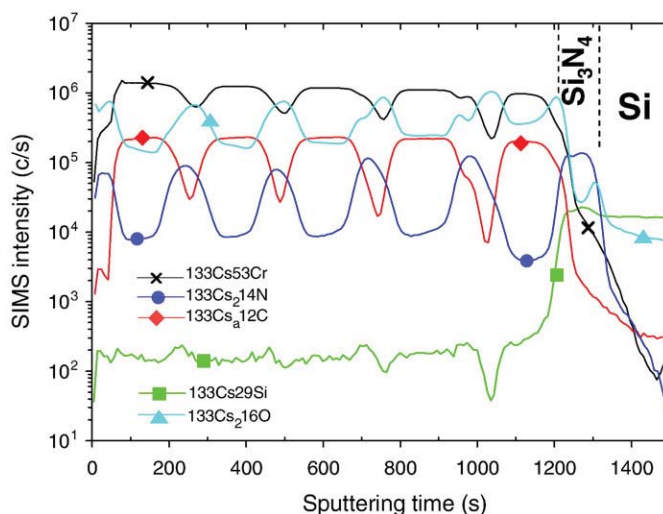
500 nm and above), a strong (200) texturation occurs. The presence of chromium oxide is detected by EPMA and XRD. This oxygen incorporation is essentially found in CrN coatings and it may result from oxygen species adsorbed in the whole set up (pipes and reactor) in spite of vacuum purge cycles and from impurities in the reactants (principally ammonia). Furthermore CrN is known to be more sensitive to oxygen than other Cr-based materials.

3.2. Multilayer CrC$_x$/CrN coatings

By monitoring the opening of the NH$_3$ valve it is possible to stack CrC$_x$ and CrN layers, resulting in multilayer CrC$_x$ / CrN coating where CrC$_x$ is the first layer deposited on the substrate. In this article, the stacking are characterised by their bilayer period λ (so-called biperiod) which is the mean thickness of a bilayer CrC$_x$ / CrN. At atmospheric pressure, it was possible to stack up to 40 layers (so called CrC$_x$/CrN-40) with a bi-period as low as 50 nm, leading to a one-micrometer-thick coating.

FEG-SEM micrography (Fig. 4) illustrates a 10 layer coating deposited on a silicon substrate with a silicon nitride sublayer as

Fig. 4. SEM-FEG of cross section view of a fractured CrC$_x$/CrN-10 coating grown at 773 K on Si substrates protected with a Si$_3$N$_4$ thin layer. The bi-period is 204 nm.
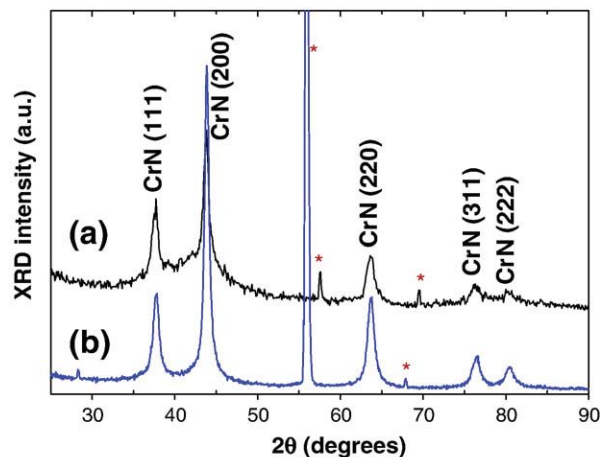

Fig. 6. Grazing angle (2°) XRD patterns of multilayer coatings grown at 773 K on Si substrates: (a) CrC$_x$/CrN-10 (10 layers with a bi-period of 204 nm); (b) CrC$_x$/CrN-40 (40 layers with a bi-period of 55 nm).
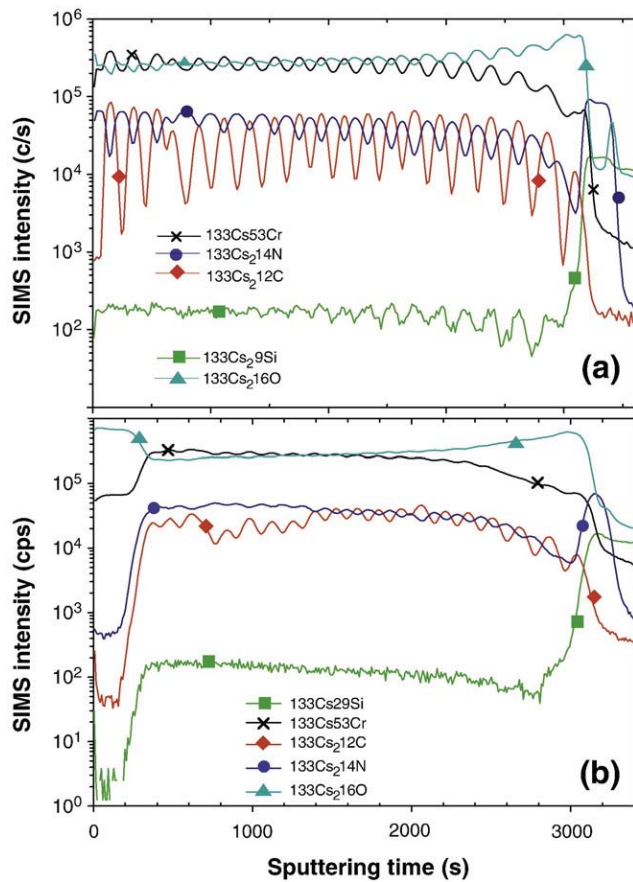
Fig. 7. SIMS depth profile of nanostructured CrC$_x$/CrN-40 layer coating with a bi-period of 55 nm: (a) as deposited; (b) after heat treatment at 973 K for 4 h under nitrogen.

3.3. Preliminary properties

Preliminary functional properties for further mechanical and tribological applications were investigated where high temperature can be involved. That is the reason why the thermal behaviour of the coating has first been studied.

A CrC$_x$/CrN-40 sample was annealed at 973 K under inert atmosphere, in order to evaluate the thermal stability of the interfaces. The 40-multilayer structure remains stable for a few hours at 973 K. After 4 h, a superficial oxidation is observed and diffusion phenomena occur, which results in smoothing the CrC$_x$/CrN interfaces (Fig. 7). This reveals a good thermal stability of the CrC$_x$/CrN interfaces in agreement with recent thermodynamic calculations which have demonstrated that they are thermodynamically stable [26].

The mechanical properties of the mono and multilayers are summarized in Table 3. Compressive stresses were measured from the curvature of the samples for all the coatings: they are close to the calculated thermal stresses. Hardness and wear resistance are improved by stacking the layers. For instance, monolithic layers exhibit hardnesses in a 14–15 GPa range whereas the multilayers reach 18–25 GPa. Moreover, the decrease of the biperiod which leads to a nanostructuration of the coatings enhances their mechanical characteristics. Nevertheless this influence seems to have limits since the hardness does not change significantly when the biperiod is reduced from 85 to 50 nm. Further experiments need to be performed to confirm this trend.

The biperiod value also influences the wear rate: when λ changes from 650 nm down to 85 nm the wear rate is reduced by 3 magnitude orders. The depth track reveals that only two layers out of 40 has been wear destroyed. The friction coefficient of the multilayers is around 0.45. Scratch test did not reveal significant difference of adherence whatever the design of the coating.

4. Conclusions

A competitive and innovative atmospheric pressure CVD process was developed for the growth of chromium-based coatings on steel substrate by combining metalorganic precursors for low temperature deposition and direct liquid injection to feed the CVD reactor with high flow rates of reactive vapours.

Monolithic as well as multilayer chromium-based coatings were deposited by DLI-MOCVD at atmospheric pressure, enabling further applications where vacuum equipment and batch operation are a lock. The growth rate and design of the coatings are easily tuned since the injectors are computer controlled.

Stacking Cr$_x$C/CrN layers with a biperiod as low as a few tens of nanometres leads to a nanostructuration of the coatings and enhances their properties in comparison with the monolithic layers. The multilayer coatings exhibit promising mechanical properties (e.g.

barrier. The contrast between the amorphous morphology of CrC$_x$ and the columnar aspect of CrN is highlighted. The interfaces are well-defined and sharp as confirmed by SIMS analysis (Fig. 5). The N and C composition depth profiles are in opposition, revealing the succession of the various layers: no interfacial diffusion is observed. SIMS measurements also confirm the incorporation of oxygen essentially in the CrN layers.

XRD analysis of the coating is in agreement with results from monolithic layers: the multilayer coatings exhibit a fcc crystalline structure resulting from CrN contribution, while the CrC$_x$ layers are still amorphous. This is clearly observed when the volume fraction of CrC$_x$ is high enough to give the broad peak around 42°, as for the monolithic layer (Fig. 6).

Table 3

Preliminary mechanical properties of multilayer and monolithic Cr-based coatings grown by DLI-MOCVD under atmospheric pressure at 773 K on stainless steel substrate.

Coatings	Thickness (nm)	λ (nm)	Residual stress (GPa)	H (GPa)	E (GPa)	Friction coefficient[a]	Depth track[a] (nm)	Wear rate[a] (mm³ N⁻¹ m⁻¹)
CrC$_x$/CrN-4	1300	650	—	—	—	0.47 ± 0.06	65	2 10⁻⁶
CrC$_x$/CrN-10	1100	220	− 1.9	18.7	225	—		–
CrC$_x$/CrN-20	850	85	—	25.0	280	0.47 ± 0.05	70	3 10⁻⁹
CrC$_x$/CrN-40	1000	50	− 2	24.1	303	0.40 ± 0.04	50	8 10⁻¹⁰
Cr	450	—	− 1.3[b]	17	270	—		–
CrC$_x$	900	—	− 0.6 ± 0.1	13.7	250	0.46 ± 0.08	60	2 10⁻⁶
CrN	1700	—	− 2[c] ± 0.1	14.8	281	0.39 ± 0.08	60	3 10⁻⁹
SS304L	—	—	—	6.9	222	[d]	4300	9 10⁻⁴

The surface roughness of all coatings is in the range 20–30 nm.
[a] Tribological pin-on-disk test against alumina.
[b] Measured for a sample with a thickness of 1.5 μm.
[c] Measured for a sample with a thickness of 1.2 μm.
[d] Not measurable because the sample was strongly abraded and the trace was very noisy.

25 GPa for hardness).The interfaces between the layers are sharp and remain stable after thermal treatment. Improvement of the process is currently in progress.

References

[1] O. Knotek, F. Löffler, G. Krämer, in: R.F. Bunshah, G.E. McGuire, S.M. Rossnagel (Eds.), Handbook of hard coatings: deposition technologies, properties and applications, 2000, p. 377.
[2] S. Veprek, M. Haussmann, S. Reiprich, L. Shizhi, J. Dian, Surf. Coat. Technol. 86–87 (1996) 394.
[3] H. Holleck, H. Schulz, Thin Solid Films 153 (1987) 11.
[4] E. Martinez, J. Romero, A. Lousa, J. Esteve, J. Phys. D: Appl. Phys. 35 (2002) 1880.
[5] E. Martinez, J. Romero, A. Lousa, J. Esteve, Surf. Coat. Technol. 163–164 (2003) 571.
[6] P.C. Yashar, W.D. Sproul, Vacuum 55 (1999) 179.
[7] K.K. Shih, D.B. Dove, Appl. Phys. Letters 61 (1992) 654.
[8] J.K. Park, Y.J. Baik, Surf. Coat. Technol. 200 (2005) 1519.
[9] U. Helmersson, S. Todorova, S.A. Barnett, J.E. Sundgren, L.C. Markert, J.E. Greene, J. Appl. Phys. 62 (1987) 481.
[10] H.C. Barshilia, A. Jain, K.S. Rajam, Vacuum 72 (2003) 241.
[11] F.B. Wu, S.K. Tien, J.G. Duh, Surf. Coat. Technol. 200 (2005) 1514.
[12] P.E. Hovsepian, D.B. Lewis, W.D. Muunz, A. Rouzaud, P. Juliet, Surf. Coat. Technol. 116–119 (1999) 727.
[13] D.B. Lewis, D. Reitz, C. Wüstefels, R. Ohser-Wiedemann, H. Oettel, A.P. Ehiasarian, P.E. Hovsepian, Thin Solid Films 503 (2006) 133.
[14] A. Lousa, J. Romero, E. Martinez, J. Esteve, F. Montala, L. Carreras, Surf. Coat. Technol. 146–147 (2001) 268.
[15] M. Berger, U. Wirklund, M. Eriksson, H. Engqvist, S. Jacobson, Surf. Coat. Technol. 116–119 (1999) 1138.
[16] M.L. Kuruppu, G. Negrea, I.P. Ivanov, L. Rohde, J. Vacuum Sci. Technol. A 16 (1998) 1949.
[17] M. Kot, W.A. Rakowski, L. Major, R. Major, J. Morgiel, Surf. Coat. Technol. 202 (2008) 3501.
[18] L. Major, J. Morgiel, B. Major, J.M. Lackner, W. Waldhauser, R. Ebner, L. Nistor, G. Van Tendeloo, Surf. Coat. Technol. 200 (2006) 6190.
[19] J. Romero, A. Lousa, E. Martinez, J. Esteve, Surf. Coat. Technol. 163–164 (2003) 392.
[20] M.A. Gomez, J. Romero, A. Lousa, J. Esteve, Surf. Coat. Technol. 200 (2005) 1819.
[21] J. Romero, E. Martinez, J. Esteve, A. Lousa, Surf. Coat. Technol. 180–181 (2004) 335.
[22] S.M. Aouadi, D.M. Schultze, S.L. Rohde, K.C. Wong, K.A.R. Mitchell, Surf. Coat. Technol. 140 (2001) 269.
[23] F. Maury, L. Gueroudji, C. Vahlas, Surf. Coat. Technol. 86/87 (1996) 316.
[24] C. Vahlas, F. Maury, L. Gueroudji, Chem. Vap. Deposition 4 (1998) 69.
[25] A. Douard, F. Maury, Surf. Coat. Technol. 200 (2006) 6267.
[26] A. Douard, C. Bernard, F. Maury, Surf. Coat. Technol. 203 (2008) 516.
[27] F. Maury, S. Delclos, D. Samelor, C. Tendero, A. Douard, M.C. Lafont, to be published.